Polarimetric Radar Interferometry

Shane R. Cloude[1], Konstantinos P. Papathanassiou*

Applied Electromagnetics, St. Andrews, KY16 9UR, Scotland, UK
*Institute for Radio Frequency Technology, DLR, D-82230, Wessling, Germany

ABSTRACT

In this paper we outline a general formulation of vector wave interferometry and then use this formulation to solve the optimisation problem for interferometric coherence. We show that this problem can be reduced to a singular value decomposition of a non-symmetric complex matrix. We then develop a stochastic scattering model for an elevated forest canopy and use it to demonstrate application of the optimisation scheme.

Keywords : Radar Interferometry, Polarimetry, Coherence, Optimisation

1. VECTOR INTERFEROMETRY

Scalar Interferometry involves forming the hermitian product of complex scalars s_1 and s_2 from two complex images 1 and 2. Of special significance is a hermitian coherency matrix J defined in equation 1

$$J = \left\langle \begin{bmatrix} s_1 \\ s_2 \end{bmatrix} \begin{bmatrix} s_1^* & s_2^* \end{bmatrix} \right\rangle = \left\langle \begin{bmatrix} s_1 s_1^* & s_1 s_2^* \\ s_2 s_1^* & s_2 s_2^* \end{bmatrix} \right\rangle \qquad -1)$$

From J we can obtain an estimate of the coherence between s_1 and s_2 by forming the scalar γ defined as

$$\gamma = \frac{|\langle s_1 s_2^* \rangle|}{\sqrt{\langle s_1 s_1^* \rangle \langle s_2 s_2^* \rangle}} \qquad 0 \le \gamma \le 1 \qquad -2)$$

The higher the coherence the better the phase estimate between complex variables s_1 and s_2. We now consider the vector generalisation of this formulation with a view to optimising γ.

We begin by defining a coherent scattering vector $\underline{k}$ as shown in equation 3, where S_{hh} is the complex scattering coefficient for h transmit and h receive polarisation etc..

$$\underline{k} = \begin{bmatrix} S_{HH} & S_{HV} & S_{VH} & S_{VV} \end{bmatrix}^T \qquad \underline{k}' = U_4 \, \underline{k} \qquad -3)$$

Under a change of scattering basis, $\underline{k}$ transforms to $\underline{k}'$ under a 4 x 4 complex unitary matrix as shown in 3. Physically such transformations correspond to changes in the selected scattering mechanism in the image [3].

There are 3 important hermitian products formed from the vectors for images 1 and 2 ($\underline{k}_1$ and $\underline{k}_2$). Two of these (T_{11} and T_{22}) are the standard 4 x 4 hermitian covariance matrices for the separate images [3]. The third is a 4 x 4

[1] Further Author information:
SRC (correspondence): Email : scloude@fges.demon.co.uk, Tel : (44) 1334 477598,Fax : (44) 1334 475570

SPIE Vol. 3120 • 0277-786X/97/$10.00

complex matrix Ω_{12}, which contains all the interferometric phase information between polarimetric channels. These matrices are defined in equation 4

$$T_{11} = < \underline{k}_1 \underline{k}_1^{*T} > \quad T_{22} = < \underline{k}_2 \underline{k}_2^{*T} > \quad \Omega_{12} = < \underline{k}_1 \underline{k}_2^{*T} > \qquad -4)$$

The generalised coherence is a function of these three matrices. In particular, we can construct a single hermitian matrix T_8 as in equation 5

$$T_8 = < \begin{bmatrix} \underline{k}_1 \\ \underline{k}_2 \end{bmatrix} \begin{bmatrix} \underline{k}_1^{*T} & \underline{k}_2^{*T} \end{bmatrix} > = < \begin{bmatrix} T_{11} & \Omega_{12} \\ \Omega_{12}^{*T} & T_{22} \end{bmatrix} > \qquad -5)$$

We can use T_8 to obtain an expression for the coherence as follows. We begin by defining complex unitary weights $\underline{w}_1$ and $\underline{w}_2$ to generate two complex scalars μ_1 and μ_2 as shown in 6.

$$\mu_1 = \underline{w}_1^{*T} \underline{k}_1 \qquad \mu_2 = \underline{w}_2^{*T} \underline{k}_2 \qquad -6)$$

These two scalars correspond to the complex scattering coefficients for scattering mechanisms $\underline{w}_1$ and $\underline{w}_2$. Equation 5 can now be combined with equation 6 to generate an expression for the 2 x 2 hermitian matrix J which decouples the $\underline{w}$ vectors and the matrix T_8 (equation 7).

$$J = \begin{bmatrix} \underline{w}_1^{*T} & \underline{0}^T \\ \underline{0}^T & \underline{w}_2^{*T} \end{bmatrix} \begin{bmatrix} T_{11} & \Omega_{12} \\ \Omega_{12}^{*T} & T_{22} \end{bmatrix} \begin{bmatrix} \underline{w}_1 & \underline{0} \\ \underline{0} & \underline{w}_2 \end{bmatrix} \qquad -7)$$

where $\underline{0}$ is a 4 x 1 zero matrix. We can now obtain a formal expression for the generalised coherence as

$$\gamma = \frac{|< \mu_1 \mu_2^{*T} >|}{\sqrt{< \mu_1 \mu_1^{*T} >< \mu_2 \mu_2^{*T} >}} \qquad 0 \le \gamma \le 1 \qquad -8)$$

Our task is to find $\underline{w}_1$ and $\underline{w}_2$ which optimise this expression based on estimates of the matrix T_8. First we consider the effects that propagation may have on the measurement of the scattering vector $\underline{k}$.

2. VECTOR WAVE PROPAGATION

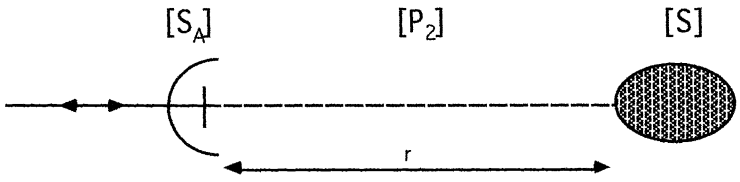

Figure 1: Propagation Distortion in Polarimetric Radar

Figure 1 shows how a matrix formulation of wave propagation may be used in Radar backscatter. In mathematical form we can write the measured scattering matrix from point A as

$$S_A = P_2 \, S \, P_2^T \qquad -9)$$

where the transpose operation follows from wave reciprocity and the propagation matrix P_2 can be written in the form of a matrix exponential as follows.

$$P_2 = \begin{bmatrix} \cos\alpha & \sin\alpha\, e^{i\delta} \\ -\sin\alpha\, e^{-i\delta} & \cos\alpha \end{bmatrix} \begin{bmatrix} e^{i\beta_1 r} & 0 \\ 0 & e^{i\beta_2 r} \end{bmatrix} = e^{i\frac{(\beta_1+\beta_2)}{2}r} (\cosh \nu\, \sigma_0 + \sinh \nu\, \underline{\sigma}.\underline{n}) \qquad - 10)$$

In equation 10 (σ_0, $\underline{\sigma}$) are the Pauli matrices defined as

$$\sigma_0 = \begin{bmatrix} 1 & 0 \\ 0 & 1 \end{bmatrix} \quad \sigma_1 = \begin{bmatrix} 1 & 0 \\ 0 & -1 \end{bmatrix} \quad \sigma_2 = \begin{bmatrix} 0 & 1 \\ 1 & 0 \end{bmatrix} \quad \sigma_3 = \begin{bmatrix} 0 & -i \\ i & 0 \end{bmatrix}$$

The angles α and δ are the Deschamps parameters of the eigenpolarisation state on the Poincaré sphere [5] and β_1 and β_2 are the *complex* wave numbers for propagation of these states (representing both attenuation and phase shifts).

The angle ν is generated by the differential constant $\nu = \beta_{diff}\, r = (\beta_1 - \beta_2)r$. Note that the interferometric information related to range dependent phase effects is contained in both the determinant and in the angle ν.

Using the matrix identity in equation 11, we can re-express equation 9 in terms of target vectors as shown in equation 12

$$A\,B\,C = A \otimes C^{T}\, \underline{b} \qquad - 11)$$

$$\underline{k}_A = P_{4A}\, \underline{k} \qquad \underline{k}_B = P_{4B}\, \underline{k} \quad \Rightarrow \quad \underline{k}_A = P_{4A}\, P_{4B}^{\dagger}\, \underline{k}_B \qquad - 12)$$

where A and B are the two antenna positions (figure 4), $\underline{k}$ is the target vector and the unitary matrices P_{4A} and P_{4B} are given by

$$\begin{aligned} P_{4A} &= e^{ir_1(\beta_1+\beta_2)}(\cosh \nu_A \sigma_0 + \sinh \nu_A \underline{\sigma}.\underline{n}_A) \otimes (\cosh \nu_A \sigma_0 + \sinh \nu_A \underline{\sigma}.\underline{n}_A) \\ P_{4B} &= e^{ir_2(\beta_1+\beta_2)}(\cosh \nu_B \sigma_0 + \sinh \nu_B \underline{\sigma}.\underline{n}_B) \otimes (\cosh \nu_B \sigma_0 + \sinh \nu_B \underline{\sigma}.\underline{n}_B) \end{aligned} \qquad - 13)$$

To generate a vector interferogram we form the complex outer product in equation 14

$$\Omega_{AB} = \underline{k}_A.\underline{k}_B^{\dagger} = P_{4A}\, \underline{k}.\underline{k}^{\dagger}\, P_{4B}{}^{\dagger} = P_{4A}\, T\, P_{4B}{}^{\dagger} \qquad - 14)$$

$$\begin{aligned} P_4 = e^{i\phi}&(\cosh^2 \nu\, \gamma_0 + \sinh \nu \cosh \nu (2n_x\gamma_1 + n_y\gamma_2 + n_z\gamma_3) \\ &+ \sinh^2 \nu (n_x^2\gamma_4 + n_y^2\gamma_5 + n_z^2\gamma_6 + n_x n_y\gamma_7 + n_x n_z\gamma_8 + 2n_y n_z\gamma_9)) \end{aligned} \qquad - 15)$$

where $\phi = (\beta_1 + \beta_2)r$ or in a simplified general form as

$$P_4 = e^{i\phi} \sum_{m=0}^{9} \alpha_m \gamma_m \qquad - 16)$$

where the 10 basis matrices γ_m are traceless hermitian and are defined in figure 2. These matrices are obtained by straightforward direct product expansions of the Pauli matrices.

Generally we must now multiply together two expressions of the form shown in equation 15 to generate equation 12. We can simplify a great deal by making one important assumption about the propagation channel. We are going to assume that the eigenpolarisations are identical for the measurements at A and B so that the only changes between the two measurement points are due to the change of range $r \rightarrow r + \Delta$. In this case the only changes from P_{4A} to P_{4B} are the determinant and angle ν

With this in mind we can write the general form of the desired unitary matrix as

$$\begin{aligned} P_{4A}\, P_{4B}{}^{\dagger} = e^{i\Delta\phi} &(\cosh \nu_A \sigma_0 + \sinh \nu_A \underline{\sigma}.\underline{n}_A) \otimes (\cosh \nu_A \sigma_0 + \sinh \nu_A \underline{\sigma}.\underline{n}_A) \\ &.(\cosh \nu_B \sigma_0 - \sinh \nu_B \underline{\sigma}.\underline{n}_A) \otimes (\cosh \nu_B \sigma_0 - \sinh \nu_B \underline{\sigma}.\underline{n}_A) \end{aligned} \quad - 17)$$

The important result to note is that when we expand this expression, we can express equation 17 as the matrix exponential of a sum of *only 3 basis matrices* so that we have the alternative and very much simplified parameterisation shown in equation 18 where the three matrices γ_1 to γ_3 are defined in figure 2.

$$\gamma_0 = \begin{bmatrix} 1 & 0 & 0 & 0 \\ 0 & 1 & 0 & 0 \\ 0 & 0 & 1 & 0 \\ 0 & 0 & 0 & 1 \end{bmatrix} \quad \gamma_1 = \begin{bmatrix} 1 & 0 & 0 & 0 \\ 0 & 0 & 0 & 0 \\ 0 & 0 & 0 & 0 \\ 0 & 0 & 0 & -1 \end{bmatrix} \quad \gamma_2 = \begin{bmatrix} 0 & 1 & 1 & 0 \\ 1 & 0 & 0 & 1 \\ 1 & 0 & 0 & 1 \\ 0 & 1 & 1 & 0 \end{bmatrix} \quad \gamma_3 = \begin{bmatrix} 0 & -i & -i & 0 \\ i & 0 & 0 & -i \\ i & 0 & 0 & -i \\ 0 & i & i & 0 \end{bmatrix} \quad \gamma_4 = \begin{bmatrix} 1 & 0 & 0 & 0 \\ 0 & -1 & 0 & 0 \\ 0 & 0 & -1 & 0 \\ 0 & 0 & 0 & 1 \end{bmatrix}$$

$$\gamma_5 = \begin{bmatrix} 0 & 0 & 0 & 1 \\ 0 & 0 & 1 & 0 \\ 0 & 1 & 0 & 0 \\ 1 & 0 & 0 & 0 \end{bmatrix} \quad \gamma_6 = \begin{bmatrix} 0 & 0 & 0 & -1 \\ 0 & 0 & 1 & 0 \\ 0 & 1 & 0 & 0 \\ -1 & 0 & 0 & 0 \end{bmatrix} \quad \gamma_7 = \begin{bmatrix} 0 & 1 & 1 & 0 \\ 1 & 0 & 0 & -1 \\ 1 & 0 & 0 & -1 \\ 0 & -1 & -1 & 0 \end{bmatrix} \quad \gamma_8 = \begin{bmatrix} 0 & -i & -i & 0 \\ i & 0 & 0 & i \\ i & 0 & 0 & i \\ 0 & -i & -i & 0 \end{bmatrix} \quad \gamma_9 = \begin{bmatrix} 0 & 0 & 0 & -i \\ 0 & 0 & 0 & 0 \\ 0 & 0 & 0 & 0 \\ i & 0 & 0 & 0 \end{bmatrix}$$

Figure 2: Basis Matrices for Polarimetric Interferometry

$$P_{4\Delta} = P_{4A}\, P_{4B}{}^{\dagger} = e^{i\Delta\phi}\, e^{i(\varepsilon_1\gamma_1 + \varepsilon_2\gamma_2 + \varepsilon_3\gamma_3)} \quad - 18)$$

This result permits us to re-write the basic equation of vector Radar interferometry in the parametric form shown in equation 19

$$\underline{k}_A = e^{i\Delta\phi}\, e^{i(\varepsilon_1\gamma_1 + \varepsilon_2\gamma_2 + \varepsilon_3\gamma_3)}\, \underline{k}_B \quad - 19)$$

where the ε_i are complex constants.

3 SIMPLIFIED VECTOR PROPAGATION MATRIX

In the above section we have developed a general theory of coherent vector wave propagation. We see that much of the complexity arises from the differential propagation constant i.e. from the difference in complex propagation between the eigenpolarisations for the medium. In many practical instances this difference will be small. To help analyse such a case we can define an equivalent differential wavelength as

$$\lambda_{diff} = \frac{\lambda_1 \lambda_2}{\lambda_2 - \lambda_1} \quad - 20)$$

which shows that as $\lambda_1 \Rightarrow \lambda_2$ then λ_{diff} tends to infinity. If we can then assume that the product $\beta_{diff}\, r << 1$ then the hyperbolic functions in 15 can be approximated by the first terms in their series representation. Physically we are restricting attention to problems where the thickness of the medium is small compared to the *differential* wavelength scale.

In this case we can use $\cosh \beta_{diff}\, r \approx 1$ and $\sinh \beta_{diff}\, r \approx \beta_{diff}\, r$ so that we can write the propagation matrix (equation 15) in the simplified form

$$P_4 = e^{i\phi}(\gamma_0 + \beta_{diff}\, r(2n_x\gamma_1 + n_y\gamma_2 + n_z\gamma_3)) \qquad -21)$$

and so the general 4 x 4 propagation matrix is of the form

$$P_4 = e^{i\phi}\begin{bmatrix} 1+2\beta_{diff}n_x r & \beta_{diff}r(n_y - in_z) & \beta_{diff}r(n_y - in_z) & 0 \\ \beta_{diff}r(n_y + in_z) & 1 & 0 & \beta_{diff}r(n_y - in_z) \\ \beta_{diff}r(n_y + in_z) & 0 & 1 & \beta_{diff}r(n_y - in_z) \\ 0 & \beta_{diff}r(n_y + in_z) & \beta_{diff}r(n_y + in_z) & 1-2\beta_{diff}n_x r \end{bmatrix} \qquad -22)$$

where r is the distance travelled, β_{diff} the complex differential wavenumber and $\underline{n}$ is a three element vector indicating the direction in Stokes space of the orthogonal eigenstates for the medium. In the simplest case we have h and v as propagation eigenstates so $\underline{n} = (1, 0, 0)$ giving

$$P_4 = e^{i\phi}\begin{bmatrix} 1+2\beta_{diff}r & 0 & 0 & 0 \\ 0 & 1 & 0 & 0 \\ 0 & 0 & 1 & 0 \\ 0 & 0 & 0 & 1-2\beta_{diff}r \end{bmatrix} \qquad -23)$$

This represents the simplest form of the vector propagation matrix in a medium with h and v as eigenstates and a thickness small compared to the differential wavelength scale. In many practical cases we may further ignore the perturbation terms on the diagonal in which case P_4 reduces to a complex scalar times the identity matrix. We now use such an approximation to generate a model for coherent vector scattering from a vegetation layer.

4. CANOPY PENETRATION MODEL

In this section we consider an electromagnetic model for the backscatter of Radar signals from forestry and other vegetation. Figure 4 shows the key elements of this model. We assume the wave propagates through a vegetation layer of thickness r_1 and then interacts with a scatterer which may be the ground, a point scatterer or a ground trunk interaction. We assume a tenuous particle cloud model for the canopy but allow the particle scattering to vary with $\underline{r}$ and for the particles to be anisotropic in shape and have different orientation distributions. We further assume the hidden scatterer is characterised by its position $\underline{r}_t$ and coherency matrix T.

In order to obtain a vector interferometric model we require an explicit expression for the 8 x 8 hermitian matrix T_8. This we can generate in 3 stages:

- Stage 1 : Propagate the wave up to range $r = r_0$.
- Stage 2 : Wave is backscattered at $r = r_0$ by a coherent vector random process $\underline{k}$
- Stage 3 : Propagate the scattered wave back to the radar using the transpose of the matrix in Stage 1

If we apply this model as shown in figure 3 then we obtain the following formal expressions for the three elements of the matrix T8.

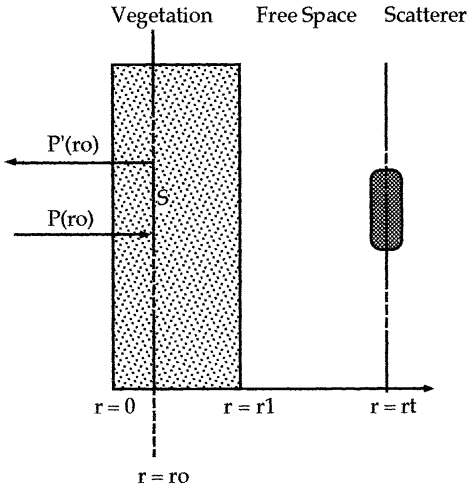

Figure 3: General Canopy Propagation Model

$$T_8 = \begin{bmatrix} T_{11} & \Omega_{12} \\ \Omega_{12}^{*T} & T_{22} \end{bmatrix} = \left\langle \begin{bmatrix} \underline{k}_1 \\ \underline{k}_2 \end{bmatrix} \begin{bmatrix} \underline{k}_1^{*T} & \underline{k}_2^{*T} \end{bmatrix} \right\rangle \qquad \begin{aligned} \underline{k}_1 &= \int_V P_{4A}(\underline{r})\, \underline{k}(\underline{r})\, d\underline{r} + P_{4A}(\underline{r}_T)\, \underline{k}_T \\ \underline{k}_2 &= \int_V P_{4B}(\underline{r})\, \underline{k}(\underline{r})\, d\underline{r} + P_{4B}(\underline{r}_T)\, \underline{k}_T \end{aligned} \qquad \text{- 24)}$$

Using the simplest scalar approximation for propagation through the canopy (equation 23 with $\beta_{diff} = 0$), we can simplify 24 so that the P matrices become complex scalars and we obtain a more "familiar" form for the complex vectors $\underline{k}_1$ and $\underline{k}_2$ as

$$\underline{k}_1 = \int_V e^{2\underline{\beta}\cdot\underline{r}_1} \underline{k}(\underline{r}_1)\, d\underline{r}_1 + e^{2\underline{\beta}\cdot\underline{r}_{1T}} \underline{k}_T \qquad \underline{k}_2 = \int_V e^{2\underline{\beta}\cdot\underline{r}_2} \underline{k}(\underline{r}_2)\, d\underline{r}_2 + e^{2\underline{\beta}\cdot\underline{r}_{2T}} \underline{k}_T \qquad \text{- 25)}$$

There remain two key issues to resolve before we can evaluate T8: the first is purely geometrical (under the scalar propagation approximation) and involves calculation of an effective propagation constant based on the range difference $\underline{r}_2$-$\underline{r}_1$ and its relation to the surface co-ordinates shown in figure 4. The second involves evaluation of the statistical polarimetric averaging implicit in the <....> brackets in equation 24. We now deal with these two issues separately.

5. EFFECTIVE PROPAGATION CONSTANT

The first problem is to relate the change in range throughout the scattering volume to the baseline radar co-ordinates and a reference surface coordinate system. Figure 4 shows the geometry, where (m,n) are the radar range and cross range co-ordinates and (z,y) the surface reference system. B_n is the normal component of the baseline and the angle θ is the mean angle of incidence onto the surface.

When we use equation 25 to evaluate T8, the matrices T_{11} and T_{22} are not sensitive to the imaginary part of the propagation constant β_i, only to the real part β_r which causes attenuation of the wave as it propagates. On the other hand the off-diagonal matrix Ω_{12} involves complex scalars of the form $\exp(-i\underline{\beta}_i .(\underline{r}_1 - \underline{r}_2))$. It is just such terms which we wish to exploit, since they give rise to sensitivity to small height changes in the scatterer position.

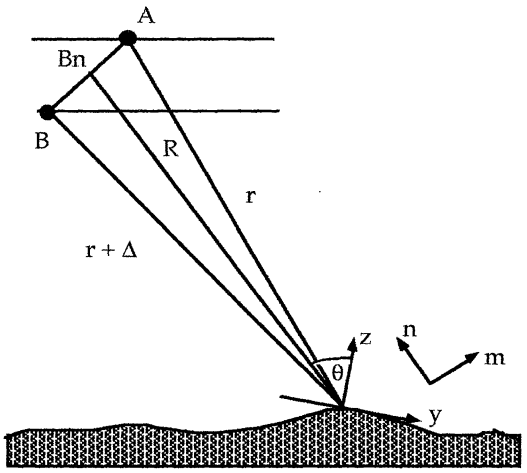

Figure 4 : Geometry for INFSAR

If we make a small angle approximation then $R >> B_n$ and the complex phase term has the simplified form

$$\exp(\frac{4\pi\,\delta\theta}{\lambda}m) \approx \exp(\frac{4\pi\,B_n}{\lambda R}m) \qquad -26)$$

where we have used the approximation $\delta\theta \approx B_n/R$ and the co-ordinate m is defined in figure 4. Note that for simplicity we are ignoring noise and temporal decorrelation effects and considering only the effects of baseline decorrelation. Noise will have no polarimetric structure and so remains unchanged in its analysis from scalar theories. Temporal decorrelation is an important effect in repeat pass interferometry which we will deal with in a separate paper.

Now transforming to the surface reference co-ordinates we can express 26 in the modified form exp(-i ϕ(y, z)) where

$$\phi(y,z) = y\left(\frac{2\beta_i B_n \cos\theta}{R} - 2\Delta\beta\sin\theta\right) + z\left(\frac{2\beta_i B_n \sin\theta}{R} + 2\Delta\beta\sin\theta\right) \qquad -27)$$

where we have further included the possibility of making a wavenumber shift $\Delta\beta$ between processing the two images [2]. As is apparent from 27, we can always remove the 'y' dependence of the phase ϕ by choosing $\Delta\beta$ based on the geometry of the system so that

$$\Delta\beta = \frac{\beta_i B_n}{R\tan\theta} \qquad -28)$$

In this case the interferometric coherence depends only on the height of the scatterers above the reference plane (the z co-ordinate in figure 5) i.e. we need consider only the volume scattering contributions as opposed to the surface contributions, which by definition lie in the reference plane and can be compensated by use of the spectral shift in 28.

To study decorrelations in the 'z' direction only, we define an effective propagation constant using 27 and 28 so that

$$\beta_z = \frac{2\beta_i B_n}{R\sin\theta} \qquad -29)$$

In this way the model in figure 3 can be reduced to a one dimensional model for wave propagation through a canopy. By employing a change of wavenumber between $\underline{k}_1$ and $\underline{k}_2$ (according to 29) we can then study the polarimetric coherence properties of such a medium.

6. POLARIMETRIC VOLUME STATISTICS

In the above analysis we showed that under a scalar approximation, propagation effects may be reduced through suitable signal processing to a simple scalar shift in wavenumber. This part is already well known in the literature [2,4]. However, the polarimetric behaviour of the canopy depends on the statistics of the $\underline{k}$ vector as a function of z. This behaviour governs the polarisation dependence of coherence and so is of prime concern to us. In this section we outline a model for such behaviour.

This model is intended to illustrate how polarimetry can make a significant difference in the observed coherence from such a volume. It is to be made as simple as possible yet must contain sufficient complexity to represent the polarimetric behaviour of a volume. For this reason we reject at this stage a full vector transport approach, although such a model may be useful for more detailed analyses [4]. Instead we adopt a simplified three level scattering model which will nonetheless contain enough physics to demonstrate how polarisation can make such a large difference to the interferometric coherence. The model is shown schematically in figure 5 and comprises the following elements:

Level 1 : The canopy is modelled by single scattering from a cloud of electrically small anisotropic particles with random orientation distribution. The particle shape may be varied from prolate (needles and twigs) through spherical to oblate (leaves). The position of these scatterers is assumed to be uniformly distributed in the range z = 0 to $z = z_1$ (see figure 5). This model gives rise to a random vector $\underline{k}_V$ defined as

$$\underline{k}_v = U(\theta)\,\underline{k}_p = a_p \begin{bmatrix} 1 & 0 & 0 \\ 0 & \cos 2\theta & \sin 2\theta \\ 0 & -\sin 2\theta & \cos 2\theta \end{bmatrix} \begin{bmatrix} \cos\alpha \\ \sin\alpha \\ 0 \end{bmatrix} \qquad -30)$$

where θ is a random variable (the particle orientation) and α is a deterministic parameter governing the particle shape ($\alpha = 0$ is a sphere $\alpha = 45^o$ a dipole). The simplest approximation is for θ to be uniformly distributed in the range 0 to π.

Level 2 : Within the canopy we assume there is a spatially localised scatterer representing the fixed branch/trunk structure. This scatterer is modelled by a deterministic scattering mechanism

$$\underline{k}_B = a_B \begin{bmatrix} \cos\alpha_B \\ \sin\alpha_B \cos\beta_B \\ \sin\alpha_B \sin\beta_B \end{bmatrix} \qquad -31)$$

where again α_B determines the type of scattering mechanism and β_B the (fixed) orientation of the scatterer. The scatterer position is assumed to be at $z_1/2$ with a uniform variation Δz where $\Delta z << z_1$ (see figure 5)

Level 3 : Beneath the canopy we model the effects of the ground or a ground/trunk interaction by locating another scattering mechanism

$$\underline{k}_G = a_G \begin{bmatrix} \cos\alpha_G \\ \sin\alpha_G \cos\beta_G \\ \sin\alpha_G \sin\beta_G \end{bmatrix} \qquad -32)$$

This mechanism can be perfectly general, ranging from a Bragg surface model to a dielectric dihedral mechanism, representing a ground-trunk multiple scattering effect. Again we assume this scatterer is located at position $z = z_g \pm \Delta z_g$ where $\Delta z_g << z_g$.

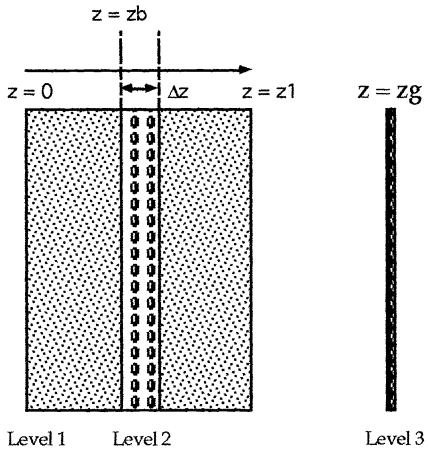

Figure 5 : Simplified 1-D Canopy Model

Note that propagation attenuation effects are simply modelled at this stage by varying the relative amplitudes a_P a_B and a_G.

This 1-D random model may now be used for numerical Monte Carlo simulation of polarimetric interferometry data. It can be used in various forms to simulate situations where the optimum coherence arises through orthogonality of the scattering mechanisms in the branch and ground layers. This case can be used as a simple test of the optimisation eigenvalue procedure to validate its performance in an 'ideal' situation before applying it to experimental data. The coherence values so obtained may also then be compared with conventional HH and VV estimates to illustrate the processing gains to be had by employing a full polarimetric sensor in interferometric applications.

In addition, the model may be used to establish the possibility of using the optimisation algorithm to obtain estimates of canopy height, without the need for multi-frequency sensor operation. This is a very important potential application, the success of which depends primarily on the difference between α_B and α_G.

7. OPTIMISATION OF COHERENCE

While much work has been carried out on optimisation in polarimetry [5], most of it has been addressed to noncoherent imagery. Hence we need to reconsider carefully the formulation of a coherent (i.e. phase preserving) optimisation problem. In order to solve the coherent optimisation problem, we must maximise the modulus of a complex Lagrangian function L defined as

$$L = \underline{w}_1^{*T}\Omega_{12}\underline{w}_2 + \lambda_1\left(\underline{w}_1^{*T}T_{11}\underline{w}_1 - 1\right) + \lambda_2\left(\underline{w}_2^{*T}T_{22}\underline{w}_2 - 1\right) \qquad -33)$$

where λ_1 and λ_2 are complex multipliers introduced so that we can maximise the numerator of equation 8 while keeping the denominator constant. We can solve this maximisation problem by setting partial derivatives to zero in the usual way. We can then solve the resulting matrix equations to obtain $\underline{w}_2$ and $\underline{w}_1$, the optimum interferometric scattering mechanisms in images 1 and 2 as

$$T_{22}^{-1}\,\Omega_{12}^{*T}\,T_{11}^{-1}\,\Omega_{12}\,\underline{w}_2 = \lambda_1\lambda_2^*\,\underline{w}_2$$
$$T_{11}^{-1}\,\Omega_{12}\,T_{22}^{-1}\,\Omega_{12}^{*T}\,\underline{w}_1 = \lambda_1\lambda_2^*\,\underline{w}_1 \qquad \text{-34)}$$

Here we have two 4 x 4 complex eigenvalue problems for the vectors $\underline{w}_1$ and $\underline{w}_2$. This constitutes a new kind of coherent decomposition theorem [3] into 6 scattering mechanisms, 3 from image 1 and 3 from image 2, which have the closest possible relation to point targets in the data.

8. SINGULAR VALUE (SVD) INTERPRETATION

If we write the two hermitian matrices T_{11} and T_{22} in terms of their eigenvalue decompositions [3], then they and their inverses can be expressed in terms of square root matrices as shown in 35

$$T_{xx} = U_x\Sigma_x U_x^{*T} = U_x\sqrt{\Sigma_x}\sqrt{\Sigma_x}U_x^{*T} = \sqrt{T_{xx}}^{*T}\sqrt{T_{xx}}$$
$$T_{xx}^{-1} = U_X\Sigma_X^{-1}U_X^{*T} = U_X\sqrt{\Sigma_X^{-1}}\sqrt{\Sigma_X^{-1}}U_X^{*T} = \sqrt{T_{XX}^{-1}}^{*T}\sqrt{T_{XX}^{-1}} \qquad \text{- 35)}$$

where x = 1,2, U is the matrix of eigenvectors and Σ is a diagonal matrix with real diagonal elements. The significance of this result lies in the fact that we can transform the complex vector $\underline{k}$ to a new basis defined by

$$\underline{k}_x' = \sqrt{\Sigma_x}U_x^{*T}\underline{k} = \sqrt{T_{xx}}\,\underline{k}_x \qquad \text{- 36)}$$

This represents a shift into the orthogonal scattering mechanisms represented by the eigenvector matrix U_X, weighted in amplitude by the reciprocal of their respective eigenvalues. Physically this represents a whitening process for the vector $\underline{k}$.

We now apply this transformation to equation 34 to obtain for the optimum weight vector $\underline{w}_2$ the modified equation 37 where Π is a 4 x 4 complex matrix. The final form of equation 37 is a classical hermitian eigenvalue problem for the eigenvectors $\underline{w}_2'$. However, the eigenvalues of this matrix (which all must be real since $\Pi^{*T}\Pi$ is hermitian) are $\lambda_1\lambda_2^*$, the same as those for the complex matrix $T_{22}^{-1}\,\Omega_{12}^{*T}\,T_{11}^{-1}\,\Omega_{12}$.

Hence we have shown that the eigenvalues in equation 34 are real and that the optimum value of the Lagrangian function L therefore corresponds to the maximum eigenvalue $\lambda_1\lambda_2^*$. Note that in equation 37 we are essentially solving the optimisation problem in a basis such that T8 has the special form shown in equation 38 where I_4 is a 4 x4 identity matrix and Π is defined in 37. In this case the modified Lagrangian function is given by equation 39, which has the form of a classical singular value decomposition for the complex matrix Π.

$$\begin{aligned}
&T_{22}^{-1}\,\Omega_{12}^{*T}\sqrt{T_{11}^{-1}}^{*T}\sqrt{T_{11}^{-1}}\,\Omega_{12}\sqrt{T_{22}^{-1}}\underline{w}_2' = \lambda_1\lambda_2^*\sqrt{T_{22}^{-1}}\underline{w}_2' \\
&\Rightarrow \sqrt{T_{22}}T_{22}^{-1}\Omega_{12}^{*T}\sqrt{T_{11}^{-1}}^{*T}\sqrt{T_{11}^{-1}}\Omega_{12}\sqrt{T_{22}^{-1}}\,\underline{w}_2' = \lambda_1\lambda_2^*\,\underline{w}_2' \\
&\Rightarrow (\sqrt{T_{22}^{-1}}^{*T}\,\Omega_{12}^{*T}\sqrt{T_{11}^{-1}}^{*T})\,(\sqrt{T_{11}^{-1}}\Omega_{12}\sqrt{T_{22}^{-1}})\,\underline{w}_2' = \lambda_1\lambda_2^*\,\underline{w}_2' \\
&\Rightarrow \quad \Pi^{*T}\Pi\,\underline{w}_2' = \lambda_1\lambda_2^*\,\underline{w}_2'
\end{aligned} \qquad \text{- 37)}$$

Physically we are then whitening the signals so as to perform speckle or 'noise' interferometry between the two images. The optimum values of speckle coherence are then given by the singular values of the matrix Π.

$$T_8' = \begin{bmatrix} I_4 & \Pi \\ \Pi^{*T} & I_4 \end{bmatrix} \quad -38)$$

$$L' = \underline{w}_1^{*T} \Pi \underline{w}_2 + \lambda_1 \left(\underline{w}_1^{*T} \underline{w}_1 - 1 \right) + \lambda_2 \left(\underline{w}_2^{*T} \underline{w}_2 - 1 \right) \quad -39)$$

9. INTERFEROMETRIC PHASE EXTRACTION

The optimum values of coherence are obtained directly as the square root of the real eigenvalues in equation 34. However we also wish to obtain estimates of the phase of the interferogram. In principle this is straightforward, from equation 6 we have

$$\phi = \arg(\mu_1 \mu_2^*) = \arg(\underline{w}_1^{*T} \underline{k}_1 \underline{k}_2^{*T} \underline{w}_2) \quad -40)$$

where $\underline{w}_1$ and $\underline{w}_2$ are obtained as eigenvectors in equation 34 and $\underline{k}_1$ and $\underline{k}_2$ are the complex scattering vectors for a given pixel in the co-registered images. However, one note of caution is required. The absolute phase of the eigenvectors is not uniquely defined by 34 and so we must add a condition which fixes the phase difference between $\underline{w}_1$ and $\underline{w}_2$ uniquely. One approach would be to set the phase of one element of the vectors to be zero, for example the first element. However, this is unsatisfactory since in some circumstances this element may be zero. A better approach is to use equation 40. Here we see that physically the interferometric phase should all be contained in the vectors $\underline{k}_1$ and $\underline{k}_2$ and hence a sensible constraint to employ is as follows

$$\arg(\underline{w}_1^{*T} \underline{w}_2) = 0 \quad -41)$$

This may be used to define the interferometric phase, apart from the case when $\underline{w}_1$ and $\underline{w}_2$ are orthogonal.

10. APPLICATION TO EXPERIMENTAL DATA

In order to solve the optimisation problem in equation 34 we first need an estimate of the matrix T_8. This we must obtain from the calibrated S matrix data itself [3]. The estimates for these parameters can be obtained by N-look complex averaging as shown in equation 42

$$T_{11} = \frac{1}{N} \sum_{i=1}^{N} \underline{k}_1 \underline{k}_1^{*T} \qquad T_{22} = \frac{1}{N} \sum_{i=1}^{N} \underline{k}_2 \underline{k}_2^{*T} \qquad \Omega_{12} = \frac{1}{N} \sum_{i=1}^{N} \underline{k}_1 \underline{k}_2^{*T} \quad -42)$$

We have analysed a mixed forestry / agricultural scene from the SIR-C data base. The optimisation was applied to L-band fully polarimetric repeat pass interferometric data in order to investigate the coherence gains to be had by employing coherent polarimetry.

Figure 6 shows the coherence values obtained as a result of the optimisation. We show four overlapping histograms of scene coherence. For reference we provide HH HV and VV coherence and then the coherence corresponding to the maximum eigenvalue of equation 34. We see that significant gains can be had by employing polarimetric processing.

11. CONCLUSIONS

In this paper we have derived a general formulation for coherent interferometry using polarised waves. We have then solved the coherent optimisation problem to obtain the optimum scattering mechanisms to use in order to extract the best phase estimates. We have further developed an electromagnetic scattering model which can be

used to explain the physical origin of these mechanisms. From this it seems that fully polarimetric, *single* frequency interferometric data is sufficient for the extraction of important forest data such as canopy height. This contrasts with other methods suggested for this task, which generally involve multi-frequency measurements. The main requirement is to obtain some canopy penetration and so low frequency operation is desirable. We have validated these ideas using L-Band data from the SIR-C mission.

In conclusion we have seen that the singular value spectrum of a 4 x 4 complex matrix may be used to decompose polarimetric interferometric problems into a set of coherent scattering mechanisms. Thus we have essentially developed a new class of coherent decomposition theory [3].

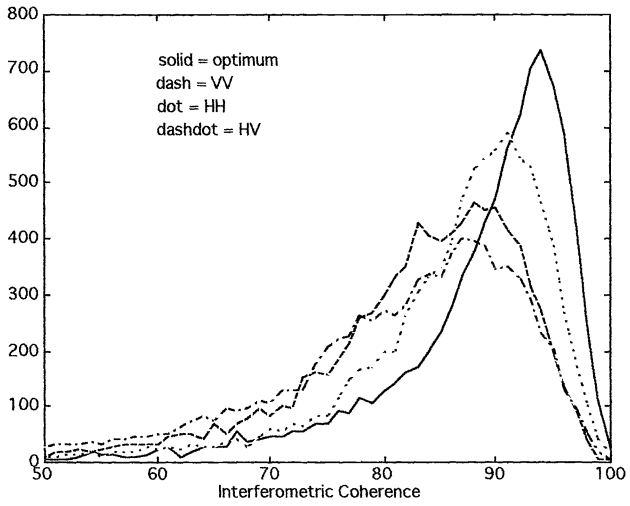

Figure 6 : Interferometric Coherence Histograms for L-Band SIR-C data

ACKNOWLEDGEMENTS

The authors wish to acknowledge the financial support of the Alexander von Humboldt Foundation, Bonn, Germany.

REFERENCES

[1] H. A. Zebker, J, Villasenor, "Decorrelation in Interferometric Radar Echoes", IEEE Transactions on Geoscience and Remote Sensing, Vol. 30 No. 5 September 1992, pp 950-959

[2] F Gatelli, A M Guarnieri, F Parizzi, P Pasquali, C Prati, F Rocca, "The wavenumber shift in SAR Interferometry", IEEE Transactions on Geoscience and Remote Sensing, Vol. 32, No. 4, July 1994, pp 855-864

[3] S. R. Cloude, E. Pottier, "A Review of Target Decomposition Theorems in Radar Polarimetry", IEEE Transactions on Geoscience and Remote Sensing, Vol. 34 No. 2 March 1996, pp 498-518

[4] R N Treuhaft, S N Madsen, M Moghaddam, J J van Zyl "Vegetation Characteristics and underlying topography from Interferometric radar", Radio Science, Vol. 31, pp 1449-1495, 1996

[5] W M Boerner, "Polarimetry in Remote Sensing and Imaging of Terrestrial and Planetary Environments", Invited Keynote Address, Proceedings of 3rd International Workshop on Radar Polarimetry (JIPR '95), IRESTE, University of Nantes, France, April 1995, pp 1-38